

# Towards Quantum Computing in Si MOS Technology: Single-shot Readout of Spin states in a FDSOI Split-Gate Device with Built-in Charge Detector

M. Urdampilleta<sup>1\*</sup>, L. Hutin<sup>2\*</sup>, B. Jadot<sup>1</sup>, B. Bertrand<sup>2</sup>, H. Bohuslavskyi<sup>2,3</sup>, R. Maurand<sup>3</sup>,  
S. Barraud<sup>2</sup>, C. Bäuerle<sup>1</sup>, M. Sanquer<sup>3</sup>, X. Jehl<sup>3</sup>, S. De Franceschi<sup>3</sup>, T. Meunier<sup>1</sup>, M. Vinet<sup>2</sup>

<sup>1</sup> Institut Néel, F-38042 Grenoble, France <sup>2</sup> CEA, LETI, Minatec Campus, F-38054 Grenoble, France

<sup>3</sup> CEA, INAC-PHELIQS, F-38054 Grenoble, France

\*e-mail: [matias.urdampilleta@neel.cnrs.fr](mailto:matias.urdampilleta@neel.cnrs.fr); [louis.hutin@cea.fr](mailto:louis.hutin@cea.fr)

## Abstract

We report the first demonstration of real-time monitoring of a single spin in a Quantum Dot (QD) using foundry-compatible Si MOS technology and a Split-Gate design with built-in charge detector. Since single-shot readout is an indispensable step in the pursuit of Si-based fault-tolerant quantum computing, this work contributes to asserting the fabrication of Si spin qubits in a MOS technology platform as a viable and promising option.

## Introduction

The building block of a quantum processor is the quantum bit (qubit) which is made out of a two-level quantum system. In contrast with a classical bit the information is encoded in a superposition of 0 and 1 (Fig. 1). Along with entanglement, this property can be harnessed by specifically designed algorithms to achieve a computational acceleration for applications such as cryptography, database search or simulation of quantum processes. In silicon-based quantum devices, the qubit is formed by the spin degree of freedom of a charge carrier (electron or hole) trapped in quantum dots. Tremendous progress has been achieved in this field in the past five years [1]. We recently demonstrated two-axis control of the first hole spin qubit in Si transistor-like structures using a CMOS technology platform [2,3]. In that proof-of-concept realization however, the qubit state was measured by averaging repeated destructive processes followed each time by qubit re-initialization. In order to perform fault-tolerant quantum computation with dynamical error correction codes [4], single-shot (real-time) detection of the spin state is required [5]. This is achieved by a spin-to-charge conversion process in combination with a charge detection measurement, which requires coupling the qubit QD to local charge sensor. Here we demonstrate this spin readout scheme in a compact device consisting of a split-gate nEET realized using SOI nanowire technology on a 300-mm fab line.

## Split-Gate devices and Quantum Dots

The fabrication flow and EM views on Fig. 2 describe the fabricated devices, which are nearly identical to conventional SOI NanoWire FETs. Following mesa patterning on 300mm undoped SOI wafers ( $T_{Si}/T_{BOX}=12\text{nm}/145\text{nm}$ ), a high-k/MG stack was deposited and patterned using hybrid DUV/E-Beam lithography to achieve a 65nm Gate pitch. A particularly large spacer (30nm SiN) is defined prior to the self-aligned ion implants. Its primary purpose is to provide sufficient access resistance to localize charges in the Gate-defined QDs, hence enabling Single Electron Transistor (SET) operation. A standard salicidation and Back-End-Of-Line process is then performed to complete the fabrication.

In the following, our device of interest has a “Split-Gate” geometry ( $W=45\text{nm}$ ;  $L_{G1}=L_{G2}=50\text{nm}$ ; inter-Gate spacing  $S_{FF}=30\text{nm}$ ) and n-type S/D doping. The electric field is strongest where the Gates wrap around the top mesa edges, hence defining “corner QDs” [6]. The spacer-protected thin undoped SOI regions on each side act as tunnel junctions providing longitudinal confinement. Each corner dot can be loaded with a small and tunable number of strongly confined electrons. With an adequate landscaping of the electrostatic potential in the channel, a third Single Electron Transistor (SET) can be formed in the middle of the mesa and between the Gates, with capacitive coupling to both QDs (Fig. 3). The DC transfer characteristic of this “built-in” SET – i.e. the gate-voltage position of its Coulomb peaks – is sensitive to any variation in the number of charges stored in either of the two corner QDs, as explained qualitatively in Fig. 4. It is thus essentially a charge detector.

## Single-Shot Detection of a Quantum Dot Charge State

Fig. 5 shows a color scale mapping of  $I_{SET}$  vs. ( $V_{G1}$ ,  $V_{G2}$ ), measured at 350mK and for  $V_{DS}=150\mu\text{V}$ . A Coulomb peak is

materialized in this two-dimensional scan by a current ridge, and its  $\sim 45^\circ$  angle indicates that the charge detector is equally coupled to  $V_{G1}$  and  $V_{G2}$ . In the following, we focus on detection on QD1. Indeed, a discontinuity is clearly visible at a given  $V_{G1}$ , which can be interpreted as the transition between two consecutive charge occupation numbers, M-1 and M, in QD1 [7]. A “read point” located on this boundary can be defined by choosing  $V_{G2}$  so that  $I_{SET}$  would be low if QD1 contained M-1 electrons, and high if it contained M electrons.

As the chemical potential of QD1 is aligned with the Fermi-level of an electron reservoir (e.g. Drain), the  $M^{\text{th}}$  electron may travel back and forth (Fig. 6(a)), causing the charge state of QD1 to fluctuate between M and M-1. This fluctuation can be tracked dynamically by monitoring  $I_{SET}$  toggling between two levels. Fig. 6(b) shows the detection in real time of single charge events occurring every few ms (tunnel rate  $\Gamma_{QD1}$ : 400Hz – 1kHz).

## Spin to Charge Conversion Using Energy-Selective Readout

As depicted in Fig. 7, when the QD contains an even number of M electrons, the  $M^{\text{th}}$  electron may occupy the same orbital as the  $M-1^{\text{st}}$  if their spins are antiparallel. In case they have the same spin however, according to Pauli’s exclusion principle, the  $M^{\text{th}}$  electron must occupy the next available orbital. As a consequence, there is an energy separation between these two spin configurations, corresponding to the orbital energy and the pairing energy. Hence, the charge state M in QD1 can be split in two levels noted  $|G\rangle$  for “ground” and  $|E\rangle$  for “excited”, depending on the spin state of the (M-1; M) electron pair.

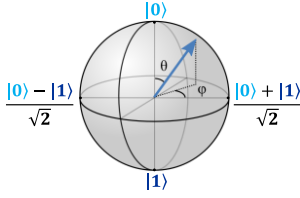
$V_{G1}$  can be adjusted so that the Drain Fermi-level lies between  $|G\rangle$  and  $|E\rangle$ . This readout strategy is called “energy selective” [8], as tunneling of an electron to the Drain is allowed from  $|E\rangle$  but it is forbidden from  $|G\rangle$  due to lack of available states below the Fermi level of the reservoir. The principle is shown in Fig. 8, as well as corresponding measured  $I_{SET}$  time traces. Since the typical time for unloading an electron from QD1 into D was determined to be  $T_{\text{unload}}=2.5\text{ms}$ , the readout measurement must be performed over a longer duration. This guarantees the appearance of a step-like signature when an electron in  $|E\rangle$  leaves QD1, whereas  $I_{SET}$  remains high when  $|G\rangle$  is occupied. This shows the successful conversion of spin information into a charge event detected by the central SET. As a sanity check, it can be useful to verify that the  $|E\rangle$  spin state cannot relax to  $|G\rangle$  within a measurement cycle. The protocol, illustrated in Fig. 9, consists in varying the latency time  $T_{\text{wait}}$  between loading an electron in QD1 and measuring  $I_{SET}$  in spin readout conditions. The probability of obtaining the “unloading” step response drops exponentially vs.  $T_{\text{wait}}$ , which means that after sufficiently long time QD1 is always in its ground state. A characteristic relaxation time  $T_1=13.5\text{ms}$  is extracted, which is consistent with typical values for electron pairs in Si [9,10].

## Conclusion

We have shown an ultra-compact device fabricated in foundry-compatible Si MOS technology, with a built-in charge detector (SET) capacitively coupled to two Gate-defined QDs. Thanks to an energy-selective detection scheme, we have demonstrated single-shot readout of the spin-state in one of the QDs, which is an essential requirement to implement fault-tolerant quantum computing. As detailed in Fig. 10, further optimization of the readout speed/fidelity trade-off can be achieved by increasing the tunnel rates (i.e. decreasing the access resistance for both the QDs and the SET) while keeping a large ( $\Gamma_{SET}-\Gamma_{QD}$ ) window. On FDSOI, the possibility of using the back-Gate as an additional handle is an asset. In particular, it can be used to tune the cross-capacitance between the SET and the QD in order to improve the readout signal. Another longer-term advantage is the perspective of reducing the parasitics by seamlessly co-integrating Si qubits with conventional control electronics circuitry.

**1-qubit state: linear combination of 2 eigenstates**

$$|\psi\rangle = \cos\left(\frac{\theta}{2}\right)|0\rangle + \sin\left(\frac{\theta}{2}\right)e^{i\varphi}|1\rangle$$



**N-qubits state:  $2^N$  arrangements of N eigenstates,  $2^N$  characteristic complex coefficients**

Fig.1: Bloch sphere representation of the quantum state space. A qubit state can be described by a linear combination of eigenstates e.g. “spin-up” and “spin-down” or “ground” and “excited”.

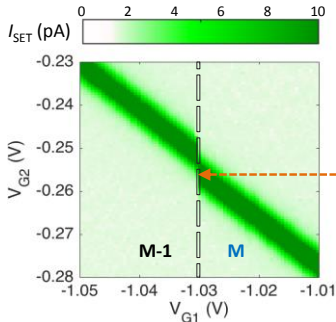


Fig.5: Left panel:  $I_{SET}$  mapping vs.  $V_{G1}$  and  $V_{G2}$ : the green trace materializes a Coulomb peak in the detector. On each side of the discontinuity (cf. dashed line), the position of the Coulomb peak vs.  $V_{G2}$  is shifted (by  $\Delta V_{peak} = C_{CROSS}/q$ ) as the charge number in QD1 changes from M-1 to M. This is visible in the right panel, which also illustrates that fixing  $V_{G2}$  at an adequate read point (cf. orange arrow) enables discriminating the M-1 and M charge states in QD1, based on the value of  $I_{SET}$  (resp. low and high). Measurements were performed at  $V_{DS} = 150\mu V$  and  $T = 350mK$ .

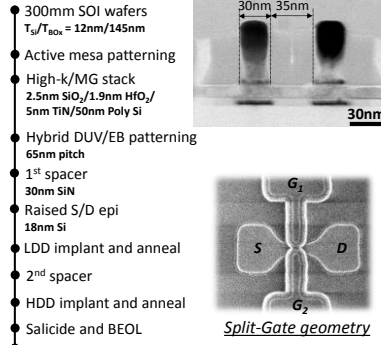


Fig.2: Left: simplified process flow. Top right: STEM view of two Gates in series (65nm pitch) showing the width of the 1<sup>st</sup> spacer. Bottom right: SEM top view of a device with Split-Gate geometry after 1<sup>st</sup> spacer definition.

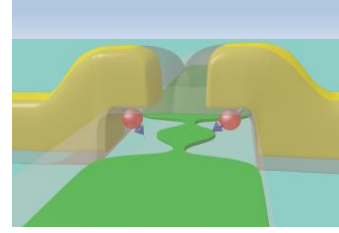


Fig.3: Artist's impression of the Split-Gate device and the built-in non-invasive detector. Quantum Dots (QDs) containing spin information are formed in the mesa corners, controlled by the wrapping Gates. Due to the electrostatic landscape in the channel, a (green) SET forms between the Gates, and is capacitively coupled to both QDs. The detection is implemented by DC current measurement through the green SET.

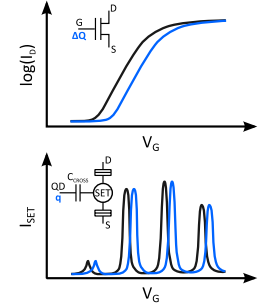


Fig.4: DC current charge detection principle. In the same way that a  $\Delta Q$  in the Gate capacitance causes a shift of the transfer characteristics in a regular FET, an elementary charge variation in the QD coupled to the SET shifts the Coulomb peaks in the latter.

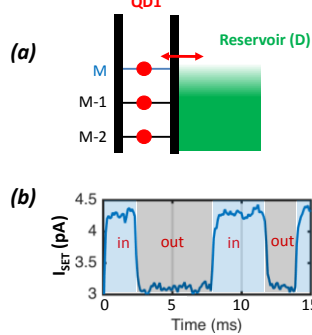


Fig.6: (a) If the chemical potential of M is aligned with the Fermi level of a reservoir (e.g. D), the charge state in QD1 may fluctuate between M and M-1. (b) As a result, at the read point defined in Fig. 5, the SET current switches in time domain between two distinct levels when the electron leaves or re-enters QD1. Statistical extractions (not shown) indicate that charge events occur on average every  $T_{load} = 1.2ms / T_{unload} = 2.5ms$ .

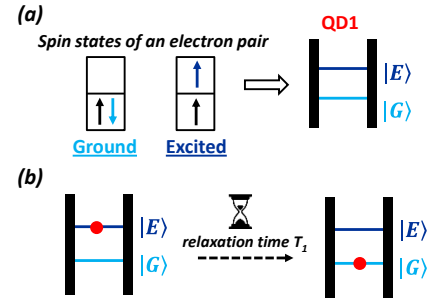


Fig.7: (a) The Pauli principle prevents two electrons with same spin from occupying the same orbital. Two configurations (Ground and Excited) are available for an even number M of electrons, and their energy difference corresponds to the orbital energy. Depending on its spin, the M<sup>th</sup> electron can occupy the QD to yield either the  $|G\rangle$  or  $|E\rangle$  state. This can be leveraged in a spin detection scheme (cf. Fig. 8). (b) The spin state of the electron pair may spontaneously change from  $|E\rangle$  to  $|G\rangle$  after a relaxation time noted  $T_1$ .

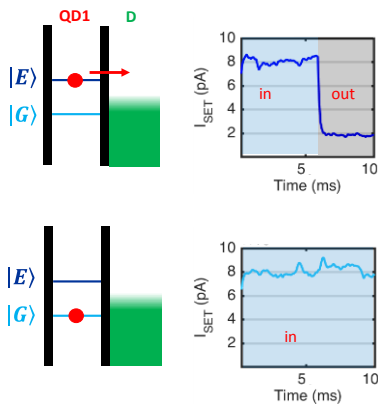


Fig.8: Spin to charge conversion scheme for single-shot readout. The Fermi energy of the reservoir is adjusted to lie between  $|E\rangle$  and  $|G\rangle$ . In such a configuration, the M<sup>th</sup> electron can only tunnel off the dot when in an excited spin state. The time domain response of  $I_{SET}$  performed over a duration longer than  $T_{unload}$  indicates whether spin tunneling has occurred, thus giving information on the electron spin state.

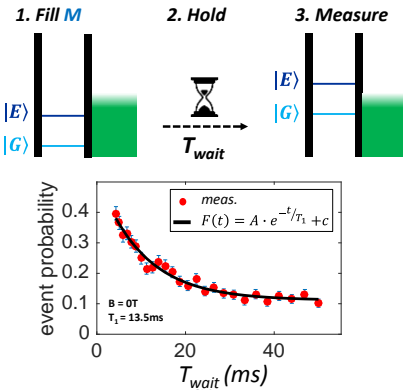


Fig.9: In order to extract the relaxation time  $T_1$ , we first load an electron in the dot, wait for a varying time  $T_{wait}$  and perform the spin measurement depicted in Fig.8. We repeat this measurement many times and plot the probability to detect an excited state is plotted vs.  $T_{wait}$ . The probability tends towards 0 eventually, and the characteristic time  $T_1 = 13.5ms$  is consistent with the expected spin relaxation times for electron pairs at zero magnetic field [10].

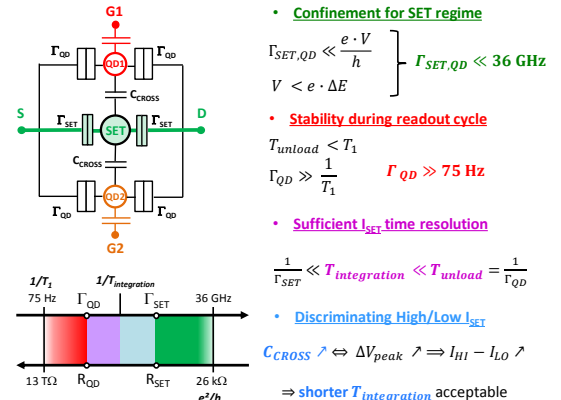


Fig.10: Schematic of the Split-Gate device. The central SET can remotely sense in real time a spin event occurring in the corner QDs. Design windows in terms of  $\Gamma$  tunnel rates, and corresponding tunnel resistance (calculated at  $V = 150\mu V$ ) are represented, based on the right-hand side considerations. Increasing the red area yields a faster readout. Maximizing the SET-Dot cross-capacitance leads to improving the readout signal and thus enables to reduce the integration time, i.e. squeeze the blue area. Tuning  $C_{CROSS}$  however requires at least another adjustment handle, e.g. the Back-Gate on FDSOI.

**References:** [1] M. Veldhorst *et al.*, Nature 526, 410 (2015). [2] L. Hutin *et al.*, VLSI (2016) [3] R. Maurand *et al.*, Nat. Commun., 7, 13575 (2016) [4] A. G. Fowler, Phys. Rev. A 86, 032324 (2012) [5] A. Morello *et al.*, Nature 467, 687 (2010) [6] S. De Franceschi *et al.*, IEDM (2016) [7] L. M. K. Vandersypen *et al.*, Appl. Phys. Lett. 85, 4394 (2004) [8] J. M. Elzerman *et al.*, Nature, 430, 431 (2004) [9] M. Xiao *et al.*, Phys. Rev. Lett., 104, 096801 (2010) [10] C. H. Yang *et al.*, Nat. Commun. 4, 2069 (2013)

**Acknowledgment** – The authors acknowledge financial support from the EU under Projects SiAM (No. 610637) and MOS-QUITO (No. 688539), the Marie Curie Fellowship within the Horizon 2020 program and the ANR-16-ACHN-0029.